Modeling the Atmospheric Boundary Layer Wind Response to Mesoscale Sea Surface Temperature Perturbations

UNIVERSITY OF MIAMI
ROSENSTIEL SCHOOL of MARINE & ATMOSPHERIC SCIENCE

UNIVERSITY OF MIAMI
CENTER for COMPUTATIONAL SCIENCE

High Performance Computing

CEOAS College of Earth, Ocean, and Atmospheric Sciences

Oregon State UNIVERSITY

Natalie Perlin[1,2], Simon de Szoeke[3], Dudley Chelton[3], Roger Samelson[3], Larry O'Neill[3], and Eric Skyllingstad[3]

[1] – RSMAS/ University of Miami (nperlin@rsmas.miami.edu); [2] – CCS/ University of Miami ; [3] – CEOAS/ Oregon State University

1. Background

Positive correlations of local surface wind anomalies with sea surface temperature (SST) anomalies at oceanic mesoscales (10–1000 km) suggest that the ocean influences atmospheric surface winds at these relatively small scales. A number of recent modeling studies investigated the mechanisms of these observed ocean-atmosphere interaction phenomena (e.g., Small et al., 2008, and references therein), and also revealed an underestimation of the surface wind response to SST by the operational global forecast models by nearly a factor of two (Chelton and Xie, 2010). The present study investigates the wind speed response to mesoscale SST variability over the Agulhas Return Current region of the Southern Ocean using the Weather Research and Forecasting (WRF) and the U.S. Navy Coupled Ocean-Atmosphere Mesoscale Prediction System (COAMPS) atmospheric models. The SST-induced wind response is assessed from eight simulations with different subgrid-scale vertical mixing parameterizations, validated using satellite QuikSCAT scatterometer winds and satellite-based sea surface temperature (SST) observations on 0.25° grids. Song et al. (2009) have previously found that the details of the mixing schemes can significantly affect the surface wind response to SST perturbations. The satellite data produce a coupling coefficient of $\boldsymbol{s_U}$ =0.42 m s^{-1} °C^{-1} for wind to mesoscale SST perturbations, and is adopted as a primary metrics for the air-sea coupling in our study, because of its greater geographical and seasonal consistency (O'Neill et al., 2012). Additional types of coupling coefficients are estimated for wind stress, or for curl and divergence of vector winds and wind stress. Vertical structure of the lower troposphere further reveals correlation between turbulent vertical mixing coefficients and coupling coefficients.

2. WRF and COAMPS models and SST forcing

Two nested domains are centered over the ARC in the South Atlantic (Fig.1), in the area featuring numerous mesoscale ocean eddies and meanders, superimposed on a large-scale meridional SST gradient in the South Indian Ocean. The models were integrated forward for 1 month from 0000 UTC 1 July to 0000 UTC 1 August 2002, and were forced at the lateral boundary at 6-h intervals with the global National Center for Environmental Prediction (NCEP) Final Analysis (FNL) Operational Global Analysis data on 1.0°×1.0° grid. The SST boundary condition was updated daily in each of the model simulations. SST fields from the NOAA Version 2 daily Optimum Interpolation (OI) analyses on a 0.25° grid were used as the lower boundary condition for the atmospheric model simulations, and for estimation of the coupling coefficients in conjunction with QuikSCAT winds. The month-long simulation period and time-averaging statistics were sufficient to obtain a robust statistical relationship between the time-averaged SST and winds. Analysis of the simulations was carried out primarily using the model results from the inner domain.

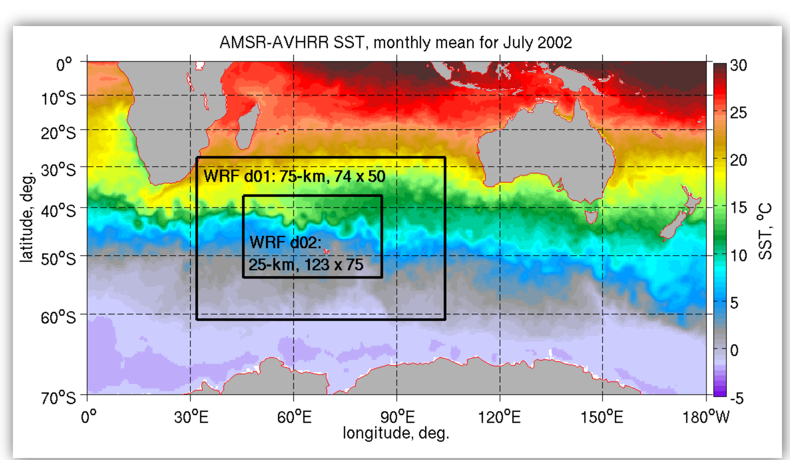

Figure 1. Monthly average of satellite sea surface temperature (SST, °C) for July 2002 from the NOAA OI 0.25° daily product generated from measurements by the Advanced Microwave Scanning Radiometer (AMSR) SST and the Advanced Very High Resolution Radiometer (AVHRR). Black rectangles outline the WRF/COAMPS outer and nested domains that have 75km and 25km grid spacing, respectively. There are 49 vertical σ layers, stretched from the 10 m above the surface up to about 18 km.

experiment name	PBL type scheme	PBL scheme reference	sfc. flux scheme (sf_sfclay_physics)
WRF_GBM	1.5-order closure	Grenier and Bretherton (2001), Bretherton et al. (2004)	MM5 Similarity (1)
WRF_MYJ	1.5-order closure	Janjić (1994, 2002)	Eta Similarity (2)
WRF_MYJ_SFCLAY	1.5-order closure	Janjić (1994, 2002)	MM5 Similarity (1)
WRF_MYNN2	1.5-order closure	Nakanishi and Niino (2006)	MM5 Similarity (1)
WRF_UW	1-1.5-order closure *	Bretherton and Park (2009)	MM5 Similarity (1)
COAMPS_ipbl=1	1.5-order closure	Mellor and Yamada (1982), Yamada (1983)	Louis (1979), COARE-2.6 (water)
COAMPS_ipbl=2	1.5-order closure	Mellor and Yamada (1982), Yamada (1983)	Louis (1979), COARE-2.6 (water)
WRF YSU	non-local-*K*	Hong, Noh and Dudhia (2006)	MM5 Similarity (1)

Table 1. List and summary of the eight numerical experiments for the study. The experiment names combine the name of the atmospheric model (WRF or COAMPS), and the conventional acronym of the boundary layer scheme used. In the WRF v3.3 release, the MYJ PBL scheme had to be used along with the "Eta similarity" surface layer scheme (sf_sfclay_physics=2). In the WRF_MYJ_SFCLAY case the MYJ_PBL was adapted to be used along with the "MM5 similarity" surface scheme (sf_sfclay_physics=1). Most of the PBL parameterizations based on so-called Mellor-Yamada type 1.5-order turbulence closure, also known as level 2-2.5 schemes (Mellor and Yamada, 1974; 1982). The term *order closure* refers to the highest order of a statistical moment of the variable for which prognostic equations are solved in a closed system of equations (Stull, 1988, Chapter 6, Table 6-1). In a 1.5-order closure, some but not all the second-moment variables are predicted, and others are parameterized with a diagnostic equation. For most of the 1.5-order schemes considered here, an additional prognostic equation is solved for the turbulent kinetic energy (TKE, $q^2/2 = (u'^2 + v'^2 + w'^2)/2$), but the other second moments (the Reynolds fluxes of the form $\overline{w'C'}$) are parameterized using the local gradient approach, as in a first-order closure.

* - The WRF_UW PBL scheme is a heavily modified version of the Grenier and Bretherton (2001) approach that is intended to improve its numerical stability for the use in climate models with longer time steps; it adapts an approach where TKE is diagnosed, rather than being prognosed, which may qualify it as lower than a 1.5-order scheme.

3. Vertical turbulent mixing parameterizations

Reynolds decomposition applied: variables are split into their mean ($\overline{\ }$) and fluctuating ($'$)components. The resulting momentum equation for the u-component of horizontal flow takes the form:

$$\frac{\partial u}{\partial t} = -u\frac{\partial u}{\partial x} - v\frac{\partial u}{\partial y} - w\frac{\partial u}{\partial z} - \frac{1}{\rho}\frac{\partial P}{\partial x} + vf - \frac{\partial\left(\overline{u'w'}\right)}{\partial z} \quad (1)$$

Subgrid-scale vertical turbulent momentum flux to be parameterized!

Vertical flux $(\overline{u'w'})$proportional to the local gradient of $\bar{u}$:

$$-\frac{\partial\left(\overline{u'w'}\right)}{\partial z} = \frac{\partial}{\partial z}\left(K_M \frac{\partial \bar{u}}{\partial z} - \gamma_c\right), \quad (2)$$

where K_M is the turbulent eddy transfer coefficient (eddy viscosity), and γ_c is the counter-gradient term.

Mellor-Yamada type PBL parameterizations in WRF and COAMPS that are 1.5- order closure, level 2-2.5 scheme (Mellor and Yamada, 1974; 1982), have an additional prognostic equation for the turbulent kinetic energy TKE ($e \equiv q^2/2 = \left(u'^2+v'^2+w'^2\right)/2$):

$$\frac{D}{Dt}\left(\frac{q^2}{2}\right) - \frac{\partial}{\partial z}\left[K_q \frac{\partial}{\partial z}\left(\frac{q^2}{2}\right)\right] = P_s + P_b - \varepsilon \quad (3)$$

, where P_s and P_b are shear and buoyant production of turbulent kinetic energy, respectively; ε is the dissipation term.

$$K_{M,H,q} = l \cdot q \cdot S_{M,H,q} \quad (4)$$

, where l is a turbulent master length scale; $S_{M,H,q}$ are stability functions for momentum, heat, and TKE, respectively.

There are different ways to parameterize turbulent eddy transfer coefficients and other related variables in vertical turbulent mixing schemes!

4. Monthly average surface wind response

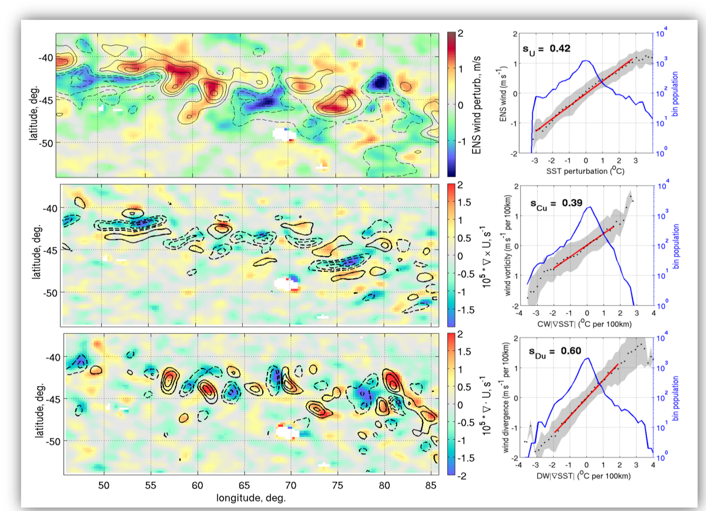

Figure 2. (**top left**) July 2002 average of QuikSCAT 10-m ENS wind perturbations (color) and satellite AMSR-E/ Reynolds OI SST perturbations (contours with an interval of 1°C with the zero contour omitted and negative contours shown as dashed lines). (**top right**) The coupling coefficient $\boldsymbol{s_U}$ estimated as a linear regression slope (red line) of wind perturbations bin-averaged on SST perturbations (black dots); the shaded gray areas show plus/minus one standard deviation of wind perturbation for each SST bin. Blue lines indicate the number of occurrences within each perturbation SST bin. (**middle row**) Similar to the top row, except for ENS wind curl (vorticity) – crosswind SST gradient perturbation fields; contour intervals of SST gradients are 1°C/100km, with negative contours dashed and the zero contour omitted. The coupling coefficient $\boldsymbol{s_{Cu}}$ is labeled on the right panel. (**bottom row**) The same as the middle row, except for ENS wind divergence – downwind SST perturbation fields; the coupling coefficient $\boldsymbol{s_{Du}}$ is labeled on the right panel.

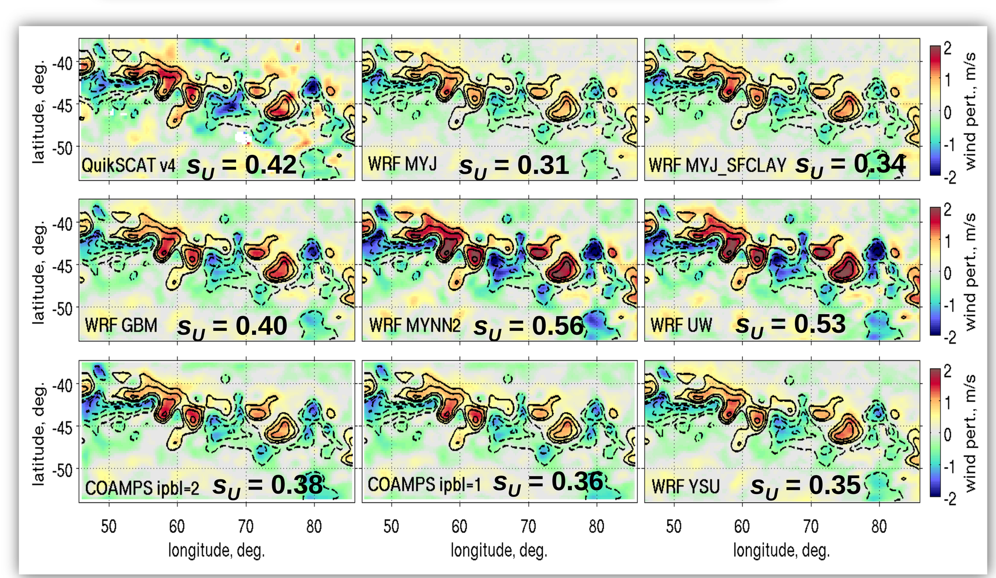

Figure 3. The July 2002 averages of 10-m ENS wind perturbations (color), and Reynolds OI SST perturbations (contours), similar to the top left panel of Fig. 2. Wind speed perturbations are shown from the (**top left**) QuikSCAT satellite wind product (v4) with 1.25°×1.25° smoothing with a loess filter; (**other panels**) the eight model simulations (WRF v3.3 or COAMPS) as indicated, with various turbulent mixing schemes. The ENS wind $\boldsymbol{U_{10mN}}$ considered here is computed as:

$$U_{10mN} = \frac{u_*}{k}\left(\ln\frac{10}{z_0}\right),$$

where the u_* is friction velocity, z_0 is the roughness length, and k = 0.4 is the von Karman constant. ENS 10-m wind coupling coefficients $\boldsymbol{s_U}$ computed similarly to Fig.2 (top right) and are labeled on each panel.

Database	s_U	s_{Cu}	s_{Du}	s_{str}	s_{Cstr}	s_{Dstr}	$\frac{s_U}{s_{U\_QS}}$	$\frac{s_{Cu}}{s_{Cu\_QS}}$	$\frac{s_{Du}}{s_{Du\_QS}}$	$\frac{s_{str}}{s_{str\_QS}}$	$\frac{s_{Cstr}}{s_{Cstr\_QS}}$	$\frac{s_{Dstr}}{s_{Dstr\_QS}}$
WRF_MYJ	0.31	0.28	0.57	0.017	1.56	2.82	0.75	0.73	0.94	0.79	0.71	0.93
WRF_MYJ_SFCLAY	0.34	0.30	0.61	0.019	1.79	3.10	0.82	0.77	1.02	0.87	0.81	1.02
WRF_YSU	0.35	0.29	0.61	0.021	1.87	3.19	0.85	0.75	1.02	0.98	0.85	1.05
COAMPS_ipbl=1	0.36	0.40	0.68	0.016	1.83	2.78	0.85	1.05	1.13	0.73	0.83	0.91
COAMPS_ipbl=2	0.38	0.42	0.82	0.017	1.84	3.19	0.91	1.10	1.36	0.79	0.84	1.05
WRF_GBM	0.40	0.38	0.74	0.024	2.35	3.82	0.96	0.98	1.23	1.08	1.07	1.26
QuikSCAT v4	0.42	0.39	0.60	0.022	2.20	3.04	1.00	1.00	1.00	1.00	1.00	1.00
WRF_UW	0.53	0.53	1.03	0.033	3.54	5.66	1.27	1.38	1.70	1.49	1.61	1.86
WRF_MYNN2	0.56	0.66	1.05	0.035	3.97	6.00	1.34	1.70	1.75	1.61	1.80	1.97

Table 2. Summary of the coupling coefficients computed for different wind variables: $\boldsymbol{s_U}$ is for ENS wind – SST perturbations (m s^{-1} °C^{-1}); $\boldsymbol{s_{Cu}}$ is for ENS wind curl (relative vorticity) – crosswind SST gradient (m s^{-1} °C^{-1}); $\boldsymbol{s_{Du}}$ is for ENS wind divergence – downwind SST gradient (m s^{-1} °C^{-1}); $\boldsymbol{s_{str}}$ is for wind stress – SST perturbations (N m^{-2} °C^{-1}), $\boldsymbol{s_{Cstr}}$ is for wind stress curl– crosswind SST perturbations (100 • N m^{-2} °C^{-1}); $\boldsymbol{s_{Dstr}}$ is for wind stress divergence – downwind SST perturbations (100 • N m^{-2} °C^{-1}). Ratios in data columns 7 -12 are between the given coupling coefficient and its corresponding estimate from QuikSCAT (QuikSCAT + NOAA OI SST). Highlighted in bold and italic font are the row with QuikSCAT coupling coefficients and the column with the wind speed coupling coefficient $\boldsymbol{s_U}$ that is used in this study as the primary metric for assessment of air-sea coupling. Rows are ordered according to the magnitude of $\boldsymbol{s_U}$ for each model simulation.

5. Vertical structure of the lower troposphere

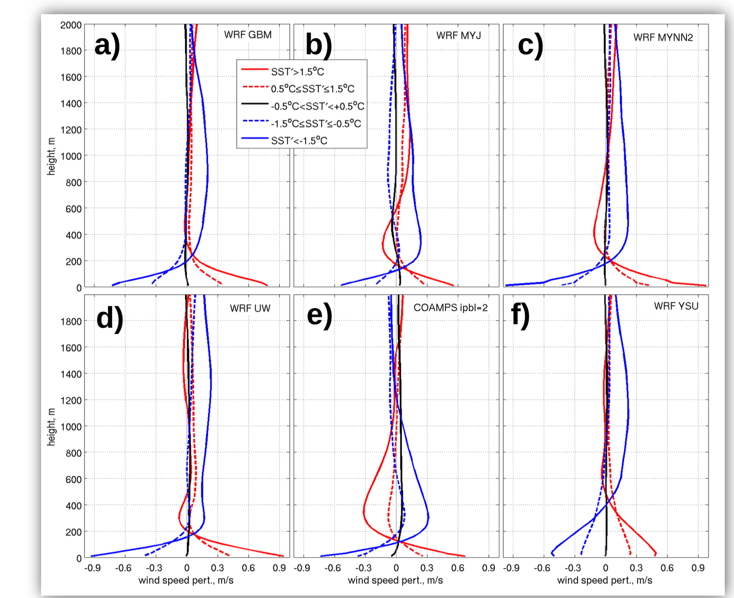

Figure 4. Average profiles of spatially high-pass filtered wind speed for ranges of SST perturbations, as indicated on the legend, for the following experiments: **(a)** WRF_GBM, **(b)** WRF_MYJ, **(c)** WRF_MYNN2, **(d)** WRF_UW, **(e)**COAMPS_ipbl2, and **(f)** WRF_YSU.

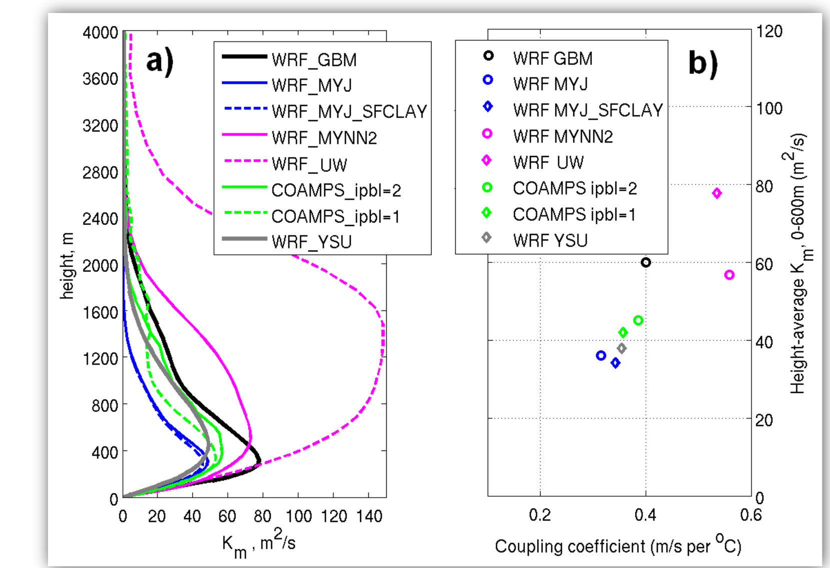

Figure 5. (**a**) Vertical profiles of monthly average eddy viscosity coefficients K_M for the nested domain for the eight experiments; (**b**) The 0–600 m vertically-averaged K_M vs. the coupling coefficient $\boldsymbol{s_U}$ for the corresponding experiment.

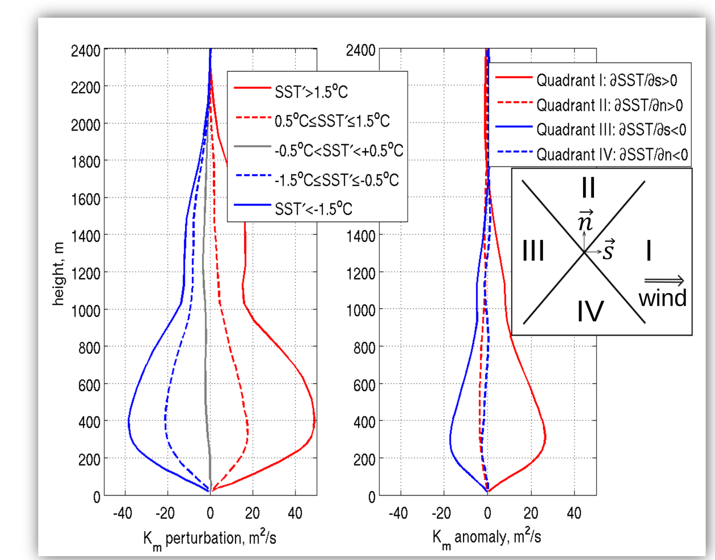

Figure 6. **(left panel)** Average profiles of eddy viscosity anomalies (K_M') from the WRF_GBM simulation for different SST perturbation ranges, where the anomaly of was determined at each level as the departure from the average at that level. **(right panel)** Monthly mean anomaly for different orientations of surface wind vector relative to the SST gradient, where the anomaly at each level was determined as the departure from the from the time- and domain-average at that level for each time step of the model simulations, after which the monthly average was computed. The vectors $\vec{s}$ and $\vec{n}$ are unit vectors in the downwind and crosswind directions, respectively (see the insert for details). Quadrants I, II, III, and IV are determined from downwind $\partial SST/\partial s$ and crosswind $\partial SST/\partial n$ components.

6. Summary

- The wind speed response to mesoscale SST variability is investigated over the Agulhas Return Current region of the Southern Ocean using the Weather Research and Forecasting (WRF) and the U.S. Navy Coupled Ocean-Atmosphere Mesoscale Prediction System (COAMPS) atmospheric models, featuring eight configurations with different turbulent mixing schemes in month-long simulation during July 2002.
- Modeled surface winds are validated using satellite QuikSCAT scatterometer winds and satellite-based sea surface temperature (SST) observations on 0.25° grids that produce a coupling coefficient of $\boldsymbol{s_U}$ =0.42 m s^{-1}°C^{-1} for wind to mesoscale SST perturbations, which is adopted as a primary metrics of the air-sea coupling in our study.
- The eight model configurations produce coupling coefficients varying from 0.31 to 0.56 m s^{-1}°C^{-1}.; the most closely matching QuikSCAT are a WRF simulation with Grenier-Bretherton-McCaa (GBM) boundary layer mixing scheme ($\boldsymbol{s_U}$ =0.40 m s^{-1}°C^{-1}), and a COAMPS simulation ($\boldsymbol{s_U}$ = 0.38 m s^{-1}°C^{-1}), with a form of Mellor-Yamada parameterizations. Additionally, the WRF_GBM simulations showed the best consistency with QuikSCAT for three of the other five coupling metrics considered in our analysis.
- The simulated wind speed coupling coefficient is found to correlate well with the height-average turbulent eddy viscosity coefficient K_M, emphasizing the importance of vertical mixing scheme details for accurate surface wind prediction.
- The details of the vertical structure of the eddy viscosity depend on both the absolute magnitude of local SST perturbations, and the orientation of the surface wind to the SST gradient.

References

• Bretherton, C.S., J.R. McCaa, and H. Grenier, 2004: A new parameterization for shallow cumulus convection and its application to marine subtropical cloud-topped boundary layers. Part I: Description and 1-D results. *Mon. Wea. Rev.*, **132**, 864-882.
• Chelton, D. B., and S.-P. Xie, 2010: Coupled ocean-atmosphere interaction at oceanic mesoscales. *Oceanog.*, **23**, 52–69.
• Grenier, H., and C. S. Bretherton, 2001: A moist PBL parameterization for large-scale models and its application to subtropical cloud-topped marine boundary layers. *Mon. Wea. Rev.*, **129**, 357-377.
• O'Neill, L. W., D.B. Chelton, and S.K. Esbensen, 2012: Covariability of surface wind and stress responses to sea-surface temperature fronts. *J. Climate*, **25**, 5916–5942.
• Perlin, N., S.P. de Szoeke, D.B. Chelton, R.M. Samelson, E.D. Skyllingstad, and L.W. O'Neill, 2014: Modeling the Atmospheric Boundary Layer Wind Response to Mesoscale Sea Surface Temperature Perturbations. *Mon. Wea. Rev.* (in revision).
• Small, R. J.; deSzoeke, S. P.; Xie, S. P.; O'Neill, L.; Seo, H.; Song, Q.; Cornillon, P.; Spall, M.; Minobe, S., 2008: Air sea interaction over ocean fronts and eddies. *Dynamics of Atmospheres and Oceans*, **45**, 274-319.
• Song, Q., D. B. Chelton, S. K. Esbensen, N. Thum, and L. W. O'Neill, 2009: Coupling between sea surface temperature and low-level winds in mesoscale numerical models. *J. Clim.*, **22**, 146-164.
• Stull, R.B., 1988: An Introduction to Boundary Layer Meteorology. *Publisher: Springer Netherlands*. 670 pp.

This research was supported by the NASA Grants NNX10AE91G and NNX10A098G.